

High-Gain Compact Circularly Polarized X-Band Superstrate Antenna for CubeSat Applications

Luiza Leszkowska^{ID}, Mateusz Rzymowski^{ID}, Member, IEEE, Krzysztof Nyka^{ID}, Senior Member, IEEE,
and Lukasz Kulas^{ID}, Senior Member, IEEE

Abstract—In this letter, a concept of a high-gain circularly polarized X-band antenna employing a partially reflecting surface (PRS) has been presented. In the initial antenna analysis, the influence of parasitic element size in the PRS structure on antenna radiation pattern parameters has been investigated and the optimal arrangement of the elements has been identified. The proposed antenna provides a wide bandwidth of return loss above 10 dB of 20% (8–9.8 GHz) and circular polarization (CP) in a frequency range 8.35–8.95 GHz. The final design is compact (62 × 62 × 22.2 mm) and lightweight (29.7 g), which makes it suitable for use not only in CubeSat X-band communication systems but also in drones and high-altitude pseudosatellite applications.

Index Terms—Antenna, circular polarization (CP), high-gain, microstrip antenna, partially reflecting surface (PRS).

I. INTRODUCTION

LONG-RANGE communication between objects such as unmanned aerial vehicles, high-altitude pseudosatellites, or satellite platforms and ground stations can be a complementary way for the terrestrial infrastructure of wireless sensor networks, especially when one is interested in monitoring large areas, e.g., in smart farming applications [1]–[4]. Such applications can provide huge surface coverage, especially when satellites operate within larger formations or constellations.

Small satellites, e.g., based on the CubeSat standard, are particularly useful in creating satellite constellations. The growing popularity of the CubeSat standard has been observed in recent years due to the real need for commercial applications for small, lightweight, and inexpensive satellites [5], [6]. CubeSat standard is based on a structure with fixed dimensions of 100 mm × 100 mm × 100 mm, which constitutes a single 1U module and a lightweight not exceeding 1.3 kg per module. These modules can be combined; however, the structure of the polypicosatellite orbital deployer, which is a container that carries the satellite into space as a rocket load, imposes a limitation on maximum CubeSat weight. As a result, apart from the need

Manuscript received March 23, 2021; revised April 25, 2021; accepted April 26, 2021. Date of publication April 29, 2021; date of current version November 16, 2021. This work was supported in part by the AFARCLOUD Project through the ECSEL Joint Undertaking under Grant 783221 and in part by the European Union's Horizon 2020 Research and Innovation Program of Austria, Belgium, Czech Republic, Finland, Germany, Greece, Italy, Latvia, Norway, Poland, Portugal, Spain, and Sweden. (*Corresponding author: L. Leszkowska*.)

The authors are with the Department of Microwave and Antenna Engineering, Faculty of Electronics Telecommunications and Informatics, Gdańsk University of Technology, 80-233 Gdańsk, Poland (e-mail: luiza.leszkowska@pg.edu.pl; mateusz.rzymowski@pg.edu.pl; krzysztof.nyka@pg.edu.pl; lukasz.kulas@eti.pg.gda.pl).

Digital Object Identifier 10.1109/LAWP.2021.3076673

for high gain and wideband operation of antennas, small size, low weight, and high efficiency have to be considered for practical space applications [7], [8].

The main task of communication modules installed on small satellites is the transmission of a high amount of data obtained from remote sensing in research missions, high-resolution surface imaging, or tracking [6]. Efficient and good quality downlink communication can be provided by antennas with circular polarization (CP) to prevent polarization mismatch due to changes in the relative orientation of the transmitting antenna toward receiving antenna. What is also particularly meaningful in the context of satellite communication. CP makes the link resistant to the impact of the Faraday effect. Relatively small dimensions and wide bandwidth necessary for the transmission of large amounts of data can be achieved for an antenna designed for the X-band [9]–[12]. Microstrip antennas meet the assumption in small satellites as to their low cost, weight, and size; however, their disadvantage is low gain. In [9], a patch antenna with printed parasitic dipoles for satellite applications using an isoflux radiation pattern has been reported. The gain of the antenna is about 6 dBi and the total dimension of the antenna is 83 mm × 83 mm × 15 mm. The common method of increasing gain is to create arrays but, as a consequence, losses in the feeding network usually cause decreased efficiency of such antennas [10], [12].

The gain of a single-patch antenna can be effectively improved by placing an additional layer above the patch [13]–[18]. The improvement of the antenna parameters can be realized by applying a set of holes in the superstrate layer [14], [15] or by placing an array of printed parasitic patches (PPs) with equal sizes and constant interelement spacing [13], [16]. In [17], varied elements, optimally selected in number and size of particular passive elements, were used to optimize gain, sidelobe level (SLL), and a beamwidth of a linearly polarized (LP) superstrate antenna. As a result, a 5.9 GHz LP superstrate antenna having only a 5 × 5 array of square patches provided a gain of 18.0 dB and SLL of –18.4 dB. An interesting solution is a transformation of polarization from LP excitation source to CP in a Fabry–Perot cavity (FPC) antenna, utilizing a high-impedance surface which allows for independent control of reflection and transmission field components inside the cavity [18]. However, this approach suffers from difficulties in obtaining axial ratio (AR) below 3 dB and return loss above 10 dB simultaneously in the wide common bandwidth.

In this letter, we have adapted the method of optimal selection of square elements for the superstrate layer introduced in [17] for LP antennas to design and manufacture a left-handed circularly polarized (LHCP) superstrate antenna for CubeSat

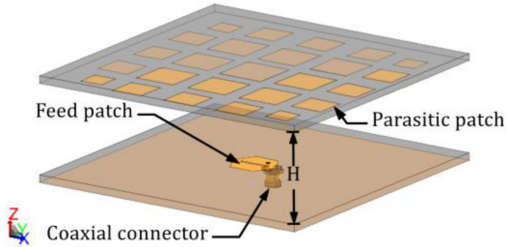


Fig. 1. Geometry of the antenna with a superstrate layer (side view), in which PPs are facing the active patch.

X-band communication. The proposed antenna has reduced cross-polarization radiation and a smaller overall dimension compared to the previous CP superstrate antenna designs [13], [19]. The result of this work is a compact lightweight antenna that was fabricated and measured. The antenna exhibits gain over 14 dBi and AR less than 3 dB bandwidth of about 6%.

II. ANTENNA CONCEPT AND DESIGN

The way the proposed antenna radiates is based on the operating principle of FPC [14]. In the presented structure, the cavity is formed between the ground plane and the array of passive metal elements printed on the dielectric layer, which acts as a partially reflecting surface (PRS), as is shown in Fig. 1. The wave exited from the active element reflects at PRS, which can cause constructive interference and result in the focusing of the beam radiated from the active patch. For the maximum gain improvement, the distance between PRS and the ground plane should be about half the free-space wavelength [14]. The design procedure of the antenna relies solely on the full-wave electromagnetic simulations in Altair FEKO and, thus, does not involve any separate considerations for the leaky-wave modes in FPC antennas.

A. Feeding Element Design

In the proposed concept, a CP single-feed hexagonal-shaped patch with a slot is used as a source element inside the cavity. The patch is printed on RO3003 substrate with a thickness of 1.52 mm, permittivity of 3.0, and loss tangent of 0.001. The patch is fed from a $50\ \Omega$ line through a coaxial probe with the feed point shifted by P_x and P_y from the center of the patch in the x- and y-axis, respectively. All dimensions of the patch are shown in Fig. 2. This type of radiating patch was chosen after designing several types of CP patch antennas that were tuned after the superstrate layer is added. In the study on proposed antenna design, we focused on the antennas where CP is provided by various means such as perturbations in the form of a slot or stub in a circular or hexagonal patch and diagonal corners truncation in a rectangular patch. Due to the same feeding method and similar dimensions, each of the investigated patches, when employed as a primary radiating element in the antenna with a superstrate layer, gives similar bandwidth and gain. Besides these two key factors, another desirable property is the even distribution of the fields reaching the superstrate layer. With this respect, the small size of the element and the symmetry of the patch are also important. A brief summary of the basic characteristics of the investigated radiating patches is given in Table I.

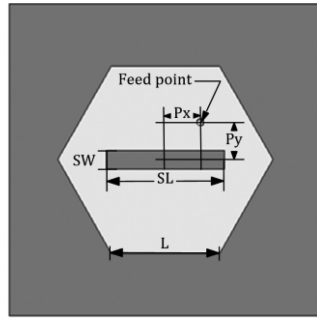


Fig. 2. Geometry of the designed microstrip patch antenna used as a feeding element with LHCP ($L = 5.34$ mm, $SL = 6.5$ mm, $SW = 0.54$ mm, $P_x = 1.9$ mm, $P_y = 2.05$ mm).

TABLE I
OVERVIEW OF THE INVESTIGATED FEEDING ELEMENTS

Type	circular patch with a slot	hexagonal patch with a slot	circular patch with a stub	rectangular patch with corners' truncation
Gain [dBi]	4.57	4.57	4.56	4.56
Size (the largest dimension)	9.8 mm (diameter)	10.7 mm (longer diagonal)	13 mm (longer diagonal)	13 mm (diameter with stub length)
HPBW [$^{\circ}$] $\phi=0^{\circ}/\phi=90^{\circ}$	110.5/111.2	110.9/111.2	108.7/112.1	111.6/106.1
Efficiency [%]	98.1	98.1	98.2	97.9

B. Superstrate Design

The superstrate layer for the proposed antenna is designed in such a way as to achieve the highest gain and wide AR parameter less than 3 dB bandwidth. For this purpose, RO3003 substrate with a thickness of 1.52 mm is placed at a distance H above the ground plane. In order to increase the reflection coefficient of this structure, an array of metal PPs is arranged on the bottom side of the layer [17]. Because the uniform size of superstrate elements proposed in [13] causes high cross-polarization radiation [19], we have used the square shape of passive elements that are distributed in a 5×5 rectangular grid symmetrical with respect to the x- and y-axis, which was proposed as optimal for an LP superstrate antenna [17]. The geometry of the proposed superstrate layer is presented in Fig. 3 where the letters indicate elements having the same size. The proposed design process relies on the observation that parasitic elements placed further from the radiating patch are smaller than the element located centrally [17]. Due to the fact that the central element in the array has the largest influence on the antenna parameters, to compensate for the phase variation, the elements' size optimization has been carried out starting from the central element (labeled A in Fig. 3). The next optimization step involved four elements (labeled B) added to the superstrate layer and their size and placement with respect to the central element has been optimized. This procedure was carried out until the last set of elements (labeled F) was reached. In each step, optimization involved the following antenna parameters: gain, AR, cross-polarization level, SLL, and beamwidth. Since AR value is particularly vulnerable to any modifications in the antenna, it was necessary to slightly adjust

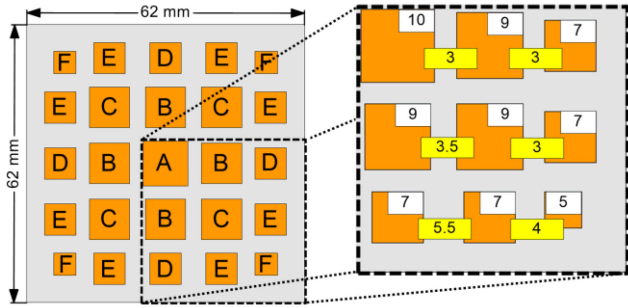


Fig. 3. Geometry of the proposed superstrate layer with dimensions (in millimeters). In the white boxes, sizes of square patches are presented, while in the yellow boxes distances between them on the dielectric layer are shown.

TABLE II
SPECIFICATION OF THE ANTENNA WITH DIFFERENT PRS CONFIGURATIONS

PP size [mm]	10	9	8	7	6	varied
S11 (-10 dB) [MHz]	1346	1303	1341	1344	1365	1381
AR 3dB [MHz]	-	450	468	383	-	600
Peak gain [dBiC]	13.7	13.6	13.4	13.4	12.5	14.5
HPBW [°] @8.6GHz	26.7	28.3	30.1	31.7	34.0	29.3
Efficiency [%]	95	95	96	95	96	95
SLL [dB] @8.6GHz	-9.7	-11.5	-13.0	-15.5	-15.7	-14.8
SLL < -10dB [MHz]	300	900	1100	1100	1500	900
Cross-pol. level [dB] @8.6GHz	-15.2	-19.3	-25.8	-19.7	-14.2	-27.3
Cross-pol. < -15dB [MHz]	160	460	480	400	-	610
Front-to-back ratio (RHC) @8.6GHz [dB]	25.6	32.8	43.3	35.0	31.2	39.8

the dimensions of the radiating patch and the air gap between the radiating patch and the superstrate layer in the final design. Although the proposed procedure is sufficiently effective for small structures to be fit in CubeSats, it may slow down for larger PRS sizes.

III. NUMERICAL RESULTS

In all simulations, the parameters of the proposed antenna with a varied size of the PPs placed within the superstrate layer were compared with the results obtained for a reference design having PPs of the same size arranged in a 5×5 array with a patch size equal to 10, 9, 8, 7, and 6 mm, and equal spacing between PPs set to 3 mm in all cases.

The simulation results, which were obtained using Altair FEKO, are summarized in detail in Table II and are presented in Figs. 4 and 5. It can easily be noticed that all the considered PRS configurations have similar S_{11} bandwidth, which is wider than 15% in every case, efficiency, and high gain above 12 dBiC. However, the biggest advantage of using the varied size of the PPs placed within the superstrate lies in high AR 3 dB bandwidth and cross-polarization radiation levels below -25 dB in a wide frequency range, which can also be seen in Fig. 5.

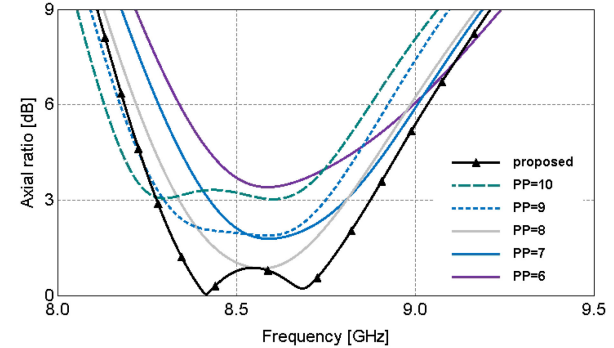


Fig. 4. Simulated AR of the antenna with different PRS configurations (see the test for explanations).

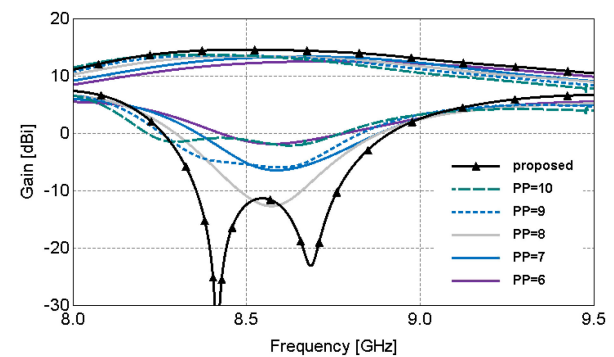


Fig. 5. Simulated LHCP and RHCP radiations of the antenna with different PRS configurations (see the test for explanations).

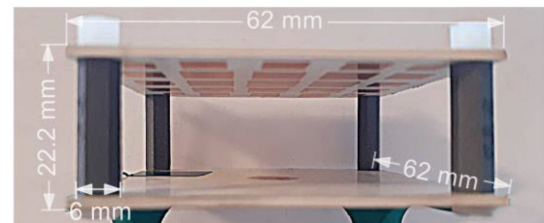


Fig. 6. Fabricated X-band antenna with the proposed superstrate layer.

IV. MEASUREMENTS

The optimized design of the proposed PRS antenna was fabricated and its prototype is presented in Fig. 6. To ensure the separation between the feeding element and the superstrate layer, four 3-D-printed plastic spacers were used to provide the exact distance. The antenna measurements were conducted in our $11.9 \text{ m} \times 5.6 \text{ m} \times 6.0 \text{ m}$ anechoic chamber and are shown in Figs. 7–10.

As it can be seen in Fig. 7, the proposed antenna is well matched in the entire bandwidth. Similarly, AR results presented in Fig. 8 match those from numerical simulations, and in the frequency range of AR below 3 dB, the reflection coefficient is maintained below -20 dB. Radiation patterns of the proposed antenna visible in Fig. 9 show good agreement with numerical simulations and illustrate the beam narrowing effect when the proposed superstrate layer is applied. By placing the additional reflecting layer, the antenna beamwidth changes from

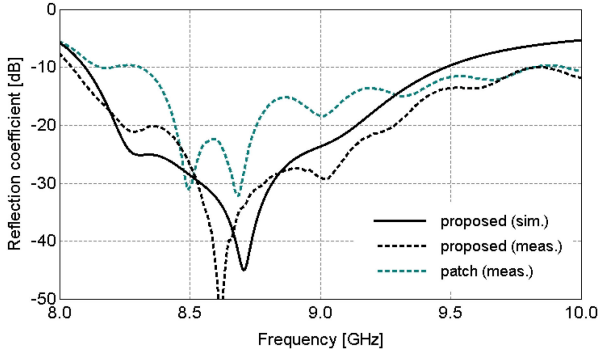


Fig. 7. Measured reflection coefficient of the proposed antenna compared to the initial antenna without additional layer.

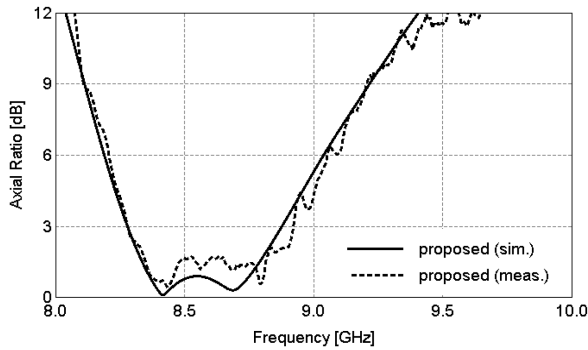


Fig. 8. Measured AR of the proposed antenna.

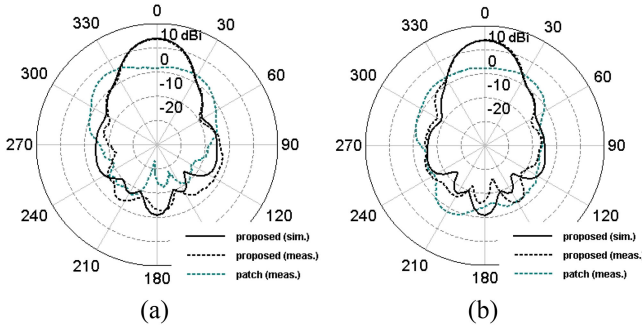


Fig. 9. Measured radiation patterns of the antenna with different PRS configurations at 8.6 GHz. (a) $\Phi = 0^\circ$ plane. (b) $\Phi = 90^\circ$ plane.

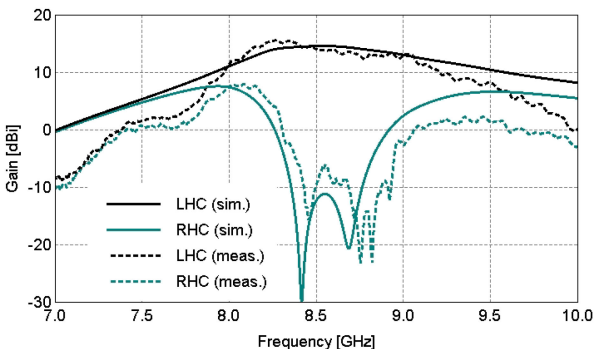


Fig. 10. Measured co- and cross-polarization level of the proposed antenna.

TABLE III
COMPARISON OF CHARACTERISTICS OF THE PROPOSED ANTENNA WITH AVAILABLE FABRICATED AND MEASURED SOLUTIONS

Ref.	Common bandwidth of AR < 3dB and S11 < -10dB [%]	Pol.	Peak gain [dBi]	SLL [dB]	Cross-pol. level [dB]	Overall size [mm ³]
[9]	~4.8 (from 8.0 to 8.4 GHz)	RHCP	6	-	-22	83 × 83 × 15
[13]	2.44 (from 8.1 to 8.3 GHz)	CP	20.5*	~-13*	-24*	170 × 170 × 21.5
[17]	~2.6 (from 5.725 to 5.875 GHz)**	linear	18	-18.4	-22.2	115 × 115 × 30
[18]	~2 (from 14.9 to 15.2 GHz)	RHCP	19.1	-20	-20	137.5 × 137.5 × 10.2
[19]	4.1* (from 8.6 to 8.95 GHz)	RHCP	16.3*	-18*	-16.4	68.5 × 68.5 × 21
Proposed	7 (from 8.28 to 8.88 GHz)	LHCP	14.6	-14.8	-27.3	62 × 62 × 22.2

*Only simulated results are available; **bandwidth of $S_{11} < -10$ dB only.

105° to 30°. In consequence, the proposed antenna can provide LHCP in the entire bandwidth with acceptable cross-polarization levels, as shown in Fig. 10. A summarizing performance comparison between the proposed antenna and the other fabricated and measured compact antennas reported in the literature is presented in Table III. The comparison shows that the proposed antenna for X-band communication outperforms other designs if the collection of all the parameters important for CubeSat applications, including S_{11} bandwidth, SLL, gain, cross-polarization level, and size, is considered.

V. CONCLUSION

In this letter, the design and realization of a compact high-gain and wide AR bandwidth superstrate CP antenna for X-band aerospace communication has been proposed. The antenna has a simple mechanical structure, which consists of an active feeding element and a superstrate layer containing passive patches, compact overall size of 62 mm × 62 mm × 22.2 mm ($1.78\lambda \times 1.78\lambda \times 0.64\lambda$), and low weight of 29.7 g, that makes it applicable to CubeSat missions. By optimizing the size of the passive elements within the superstrate layer, an appropriate phase distribution can be reached that, in turn, increases gain, widens AR 3 dB bandwidth, and improves cross-polarization suppression in the wide frequency bandwidth. As a result, the proposed antenna can also be used in systems in which the two orthogonal antennas are used to increase the bandwidth or for frequency reuse within the same satellite.

ACKNOWLEDGMENT

The authors would like to thank the Academic Computer Centre in Gdansk, Poland (TASK), where all the calculations were carried out.

REFERENCES

- [1] I. Bhakta, S. Phadikar, and K. Majumder, "State-of-the-art technologies in precision agriculture: A systematic review," *J. Sci. Food Agriculture*, vol. 99, 2019, Art. no. 4878.
- [2] S. Candiago, F. Remondino, M. De Giglio, M. Dubbini, and M. Gattelli, "Evaluating multispectral images and vegetation indices for precision farming applications from UAV images," *Remote Sens.*, vol. 7, no. 4, 2015, Art. no. 4026.
- [3] T. Adão *et al.*, "Hyperspectral imaging: A review on UAV-based sensors data processing and applications for agriculture and forestry," *Remote Sens.*, vol. 9, no. 11, 2017, Art. no. 1110.
- [4] P. Horstrand, R. Guerra, A. Rodríguez, M. Díaz, S. López, and J. F. López, "A UAV platform based on a hyperspectral sensor for image capturing and on-board processing," *IEEE Access*, vol. 7, pp. 66919–66938, 2019.
- [5] R. Sandau, "Status and trends of small satellite missions for earth observation," *Acta Astronautica*, vol. 66, no. 1/2, pp. 1–12, 2010.
- [6] R. N. Simons, "Applications of nano-satellites and cube-satellites in microwave and RF domain," in *Proc. Int. Symp. IEEE MTT-S Microw.*, Phoenix, AZ, USA, Jul. 2015, pp. 1–4.
- [7] F. E. Tubbal, R. Raad, and K. W. Chin, "A survey and study of planar antennas for pico-satellites," *IEEE Access*, vol. 3, pp. 2590–2612, 2015.
- [8] Y. Rahmat-Samii, V. Manohar, and J. M. Kovitz, "For satellites, think small, dream big: A review of recent antenna developments for cubesats," *IEEE Antennas Propag. Mag.*, vol. 59, no. 2, pp. 22–30, Apr. 2017.
- [9] J. Fouany *et al.*, "New concept of telemetry X-band circularly polarized antenna payload for cubesat," *IEEE Antennas Wireless Propag. Lett.*, vol. 16, pp. 2987–2991, 2017.
- [10] K. N. Khac *et al.*, "A design of circularly polarized array antenna for X-band cubesat satellite communication," in *Proc. Int. Conf. Adv. Technol. Commun.*, 2018, pp. 53–56.
- [11] F. Kurniawan, J. T. S. Sumantyo, Mujtahid, and A. Munir, "Effect of truncation shape against axial ratio of left-handed circularly polarized X-band antenna," in *Proc. 15th Int. Conf. Qual. Res., Int. Symp. Electr. Comput. Eng.*, 2017, pp. 83–86, doi: [10.1109/QIR.2017.8168457](https://doi.org/10.1109/QIR.2017.8168457).
- [12] M. A. Rahman, Q. D. Hossain, M. A. Hossain, E. Nishiyama, and I. Toyoda, "Design of an X-band microstrip array antenna for circular polarization," in *Proc. 8th Int. Conf. Electr. Comput. Eng.*, 2014, pp. 184–187.
- [13] G. Ganaraj, C. Kumar, V. S. Kumar, and Shankaraiah, "High gain circularly polarized resonance cavity antenna at X-band," in *Proc. IEEE Int. Conf. Antenna Innov. Mod. Technol. Ground, Aircr. Satell. Appl.*, 2017, pp. 1–5.
- [14] G. V. Trentini, "Partially reflecting sheet arrays," *IRE Trans. Antennas Propag.*, vol. AP-4, no. 4, pp. 666–671, Oct. 1956.
- [15] M. Asaadi and A. Sebak, "Gain and bandwidth enhancement of 2×2 square dense dielectric patch antenna array using a Holey superstrate," *IEEE Antennas Wireless Propag. Lett.*, vol. 16, pp. 1808–1811, 2017.
- [16] Z. M. Razi and P. Rezaei, "Fabry–Perot cavity antenna based on capacitive loaded strips superstrate for X-band satellite communication," *Adv. Radar Syst. J.*, vol. 2, pp. 26–30, 2013.
- [17] R. Gupta and J. Mukherjee, "Effect of superstrate material on a high-gain antenna using array of parasitic patches," *Microw. Opt. Technol. Lett.*, vol. 52, pp. 82–88, 2010.
- [18] R. Orr, G. Goussetis, and V. Fusco, "Design method for circularly polarized Fabry–Perot cavity antennas," *IEEE Trans. Antennas Propag.*, vol. 62, no. 1, pp. 19–26, Jan. 2014.
- [19] L. Leszkowska, M. Rzymowski, K. Nyka, and L. Kulas, "Simple superstrate antenna for connectivity improvement in precision farming applications," in *Proc. IEEE Int. Symp. Antennas Propag. North Amer. Radio Sci. Meeting*, pp. 1923–1924, 2020.